Electrical properties and stability against DC accelerated aging stress of ZPCCE-based varistor ceramics

CHOON-WOO NAHM
Department of Electrical Engineering, Dongeui University, Busan 614-714, Korea
E-mail: cwnahm@dongeui.ac.kr

The electrical properties and their stability of varistor ceramics composed of ZnO–Pr_6O_{11}–CoO–Cr_2O_3–Er_2O_3 systems were investigated as a function of Er_2O_3 content and sintering time. The varistor ceramics sintered for 1 h exhibited high nonlinear properties, with the nonlinear exponent close to 50. But the others, except for the varistor doped with 0.5 mol % Er_2O_3, exhibited very poor stability against d.c.-accelerated aging stress due to very low density. On the other hand, the varistors sintered for 2 h exhibited a more or less low nonlinear exponent, compared with those for 1 h, whereas their stability for d.c. stress was greatly improved. In particular, the varistor doped with 2.0 mol % exhibited not only high nonlinearity, with the nonlinear exponent of 47.4 and a leakage current of 1.8 μA, but also excellent stability, in which under DC accelerated aging stress such as 0.95 $V_{1\,mA}$/150 °C/12 h, the variation rate of varistor voltage, nonlinear exponent, and leakage current are − 0.54 %, − 4.41 %, and + 155.56 %, respectively.

1. Introduction

Zinc oxide (ZnO) varistors are ceramic semiconductor devices manufactured by sintering ZnO powder with small amounts of minor additives necessarily containing varistor-forming oxides such as Bi_2O_3, Pr_6O_{11}, V_2O_5, BaO, and so on. The microstructure of ZnO varistor ceramics consists of semiconducting n-type ZnO grains surrounded by very thin insulating intergranular layers, distributing a three-dimensional series-parallel network through the entire bulk [1, 2].

ZnO varistors exhibit highly nonlinear voltage–current (V–I) properties expressed by the relation $I = KV^{\alpha}$, where K is a constant and α is a nonlinear exponent, which characterizes nonlinear properties of varistors. Therefore, they are extensively used as surge absorbers in electronic circuits, devices, and surge arresters in electric power lines, such as transmission and distribution lines [1, 2]. These electrical nonlinear properties essentially are attributed to double Schottky barriers (DSBs) at the grain boundaries, containing many trap states [3, 4]. It should be pointed out that pure ZnO ceramics sintered exhibit ohmic V–I characteristics. This is because no active grain boundaries exist.

The majority of commercial ZnO varistors are Bi_2O_3-based varistors where Bi_2O_3 is used as the varistor-forming oxide (VFO). It is well known that they reveal excellent varistor properties. However, Bi_2O_3-based ZnO varistor ceramics have a few drawbacks due to Bi_2O_3 having both high volatility and reactivity [5]. To overcome these problems, recently, Pr_6O_{11}-based ZnO varistor ceramics are being actively studied for the effect of the variables, such as the kind and amount of additives, composition ratio, and sintering temperature on the electrical properties [6–18]. Most of the studies on Pr_6O_{11}-based varistor ceramics have been limited to the ternary system ZnO–Pr_6O_{11}–CoO and furthermore, on their stability with stress has been reported [6–8].

Recently, Nahm *et al*. [11–13] have reported that the varistor ceramics added with rare-earth metal oxide to the ternary system ZnO–Pr_6O_{11}–CoO exhibited relatively high nonlinearity and high stability. However, such varistor ceramics never exceeded 40 in their nonlinear exponent. More recently, ZnO varistor ceramics with Cr_2O_3 added to the quaternary system ZnO–Pr_6O_{11}–CoO–Er_2O_3 have exhibited more improved nonlinearity and stability [14–18].

The purpose of this study is to investigate the electrical properties, such as V–I and C–V characteristics, and their stability for d.c.-accelerated aging stress of ZnO–Pr_6O_{11}–CoO–Cr_2O_3–Er_2O_3-based (ZPCCE) varistor ceramics with Er_2O_3 content and sintering time. And the correlation between densification of ceramics and stability of V–I characteristics according to Er_2O_3 content and sintering time discussed.

2. Experimental procedure

2.1. Sample preparation

Reagent-grade raw materials with a composition ratio of (98–x) mol % ZnO, 0.5 mol % Pr_6O_{11}, 1.0 mol % CoO, 0.5 mol % Cr_2O_3, x mol % Er_2O_3 ($x = 0.5$–2.0) were used as the starting materials for ZPCCE-based varistor

ceramics. Raw materials were mixed by ball milling with zirconia balls and acetone in a polypropylene bottle for 24 h. The mixture was dried at 120 °C for 12 h and calcined in air at 750 °C for 2 h. The calcined mixture was pulverized using an agate mortar/pestle and after 2 wt % polyvinyl alcohol (PVA) binder addition, granulated by sieving through a 200-mesh screen to produce the starting powder. The powder was uniaxially pressed into discs 10 mm in diameter and 2 mm in thickness at a pressure of 80 MPa. The discs were covered with raw powder in an alumina crucible, sintered at 1345 °C in air for 1–2 h. The heating and cooling rates were $4\,^{\circ}\mathrm{C\,min^{-1}}$. The sintered samples were lapped and polished to 1.0 mm thickness. The size of the final samples was about 8 mm in diameter and 1.0 mm in thickness. The silver paste was coated on both faces of samples and the ohmic contact of electrodes was formed by heating at 600 °C for 10 min. The size of electrodes was 5 mm in diameter. Referentially, the three samples sintered within the same crucible indicate little different data. The medium among them was selected for measurement. The reproducibility based on parameters was relatively good, within a few percent differences.

2.2. *V–I* characteristics measurement

The voltage–current (V–I) characteristics of ZPCCE varistor ceramics were measured by stepping up the linear stair voltage in increments of 0.3–0.5 V using a programmable Keithley 237 V–I source/measure unit. To avoid joule heating of varistors, the varistors were applied up to $50\,\mathrm{mA\,cm^{-2}}$. The varistor voltage ($V_{1\,\mathrm{mA}}$) was measured at $1.0\,\mathrm{mA\,cm^{-2}}$ and the leakage current (I_ℓ) was defined as the current at 0.80 $V_{1\,\mathrm{mA}}$. In addition, the nonlinear exponent (α) is defined by $\alpha = 1/(\log E_2 - \log E_1))$, where E_1 and E_2 are the electric fields corresponding to 1.0 and $10\,\mathrm{mA\,cm^{-2}}$, respectively.

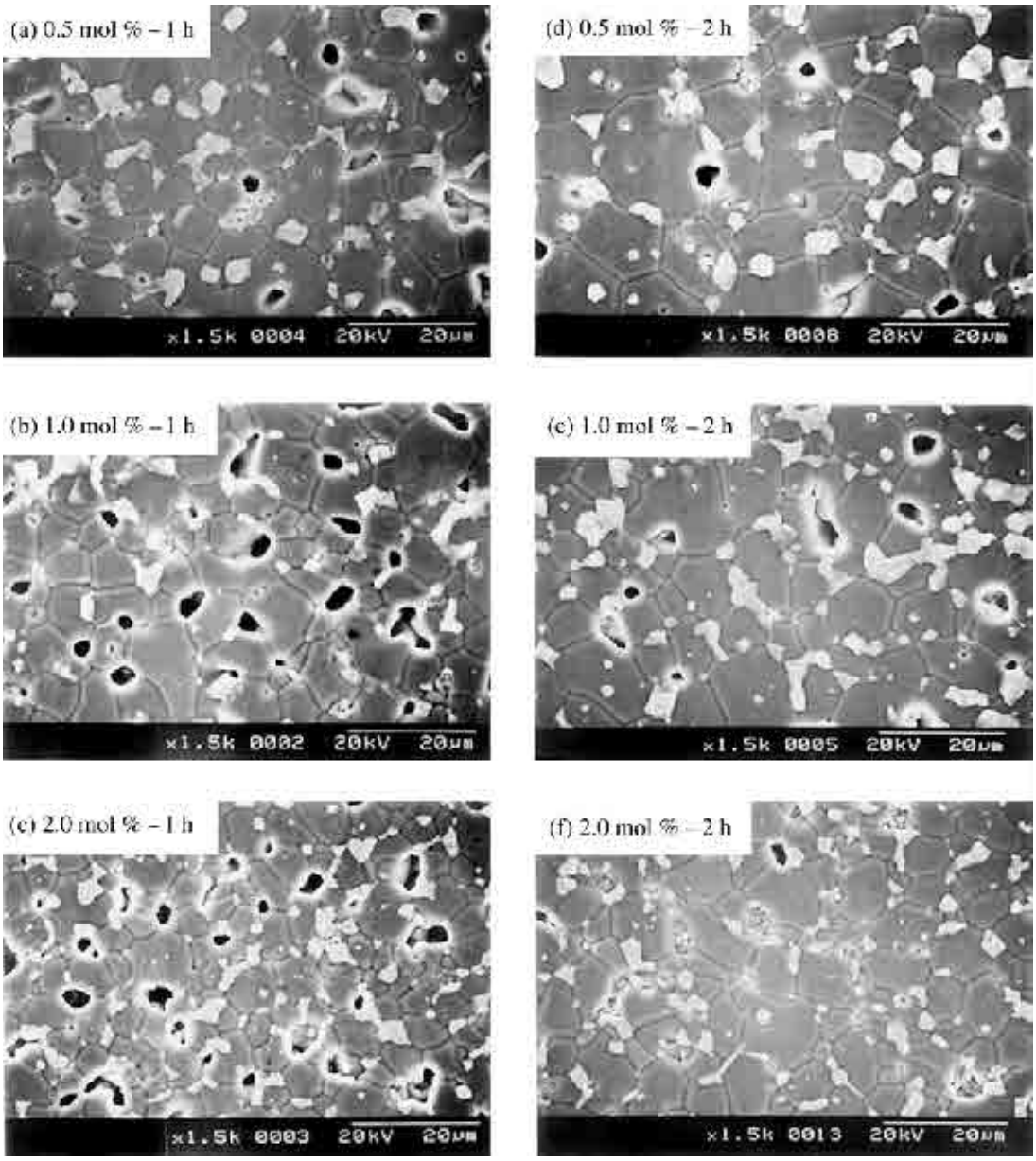

Figure 1 SEM micrographs of ZPCCE varistor ceramics versus Er_2O_3 content and sintering time.

2.3. *C–V* characteristics measurement

The capacitance–voltage (C–V) characteristics of ZPCCE varistor ceramics were measured at 1 kHz with the variable applied bias in the pre-breakdown region of the V–I characteristics using a QuadTech 7600 RLC meter and a Keithley 617 electrometer. The donor concentration (N_d) of ZnO grains and the barrier height (ϕ_b) at the grain boundary were determined from the slope and intercept of the straight line, respectively, using the equation $(1/C_b - 1/2C_{bo})^2 = 2(\phi_b + V_{gb})/q\varepsilon N_d$ proposed by Mukae *et al.* [19], where C_b is the capacitance per unit area of a grain boundary, C_{bo} is the value of C_b when $V_{gb} = 0$, V_{gb} is the applied voltage per grain boundary, q is the electronic charge, ε is the permittivity of ZnO ($\varepsilon = 8.5\varepsilon_o$). The density of interface states (N_t) at the grain boundary was determined by the equation [19] $N_t = (2\varepsilon N_d \phi_b/q)^{1/2}$ using the value of the donor concentration and barrier height obtained above. Once the donor concentration and barrier height are known, the depletion layer width (t) of either side at the grain boundaries was determined by the equation $N_d t = N_t$ [20].

2.4. Stability tests

The stability tests were performed under the five DC accelerated aging stress states, such as 0.80 $V_{1\,mA}$/90 °C/12 h in the first stress, (0.80 $V_{1\,mA}$/90 °C/12 h) + (0.85 $V_{1\,mA}$/115 °C/12 h) in the second stress, (0.80 $V_{1\,mA}$/90 °C/12 h) + (0.85 $V_{1\,mA}$/115 °C/12 h) + (0.90 $V_{1\,mA}$/120 °C/12 h) in the third stress, (0.80 $V_{1\,mA}$/90 °C/12 h) + (0.85 $V_{1\,mA}$/115 °C/12 h) + (0.90 $V_{1\,mA}$/ 120 °C/12 h) + (0.95 $V_{1\,mA}$/125 °C/12 h) in the fourth stress, and (0.80 $V_{1\,mA}$/90 °C/12 h)+ (0.85 $V_{1\,mA}$/115 °C/12 h) + (0.90 $V_{1\,mA}$/120 °C/12 h)+ (0.95 $V_{1\,mA}$/125 °C/12 h) + (0.95 $V_{1\,mA}$/150 °C/12h) in the fifth stress. And at the same time, the leakage current during the stressing time was monitored at intervals of 1 min by a Keithley 237 V–I source/measure unit.

2.5. Microstructure examination

Either surface of samples on which electrical measurement had been finished was lapped and ground with SiC paper and polished with 0.3 μm Al_2O_3 powder to a mirror-like surface. The polished samples were thermally etched at 1100–1150 °C for 10–30 min. The surface microstructure was examined by a scanning electron microscope (SEM, Hitachi S2400, Japan). The average grain size (d) was determined by the lineal intercept method [21], given by $d = 1.56L/MN$, where L is the random line length on the micrograph, M is the magnification of the micrograph, and N is the number of the grain boundaries intercepted by lines. The compositional analysis of the selected areas was determined by an attached energy dispersion X-ray analysis (EDAX) system. The crystalline phases were identified by an X-ray diffractometry (XRD, Rigaku D/max 2100, Japan) using CuK_α radiation. The density (ρ) of ZPCCE varistor ceramics was measured by the Archimedes method.

3. Results and discussion

Fig. 1 shows SEM micrographs of ZPCCE varistor ceramics for Er_2O_3 content and sintering time. It was found that the microstructure of ZPCCE varistor ceramics is not different from that of ZPCE varistor ceramics [13] with no Cr_2O_3, which consists of ZnO grains, and Er- and Pr-rich intergranular layers. Er oxide and Pr oxide were found to coexist at the grain boundaries and the nodal points as if they were a single phase. It was observed by SEM that as the Er_2O_3 content is increased, the intergranular phase was gradually more distributed at the grain boundaries and particularly the nodal points.

Fig. 2 shows the variation of the average grain size and density for various ZPCCE varistor ceramics with Er_2O_3 content and sintering time. The detailed microstructural parameters, including the average grain size (d), density (ρ), shrinkage (S), and porosity (P) are summarized in Table I. With increasing Er_2O_3 content, the average grain size of ceramics sintered for 1 h was decreased in the range of 12.6–6.4 μm and 14.1–8.5 μm for 2 h. Therefore, the Er_2O_3 was found to act as an inhibitor of grain growth. It was found that the density of ceramics sintered for 1 h is in the range of 5.22–5.42 g cm^{-3} corresponding to 90.3–93.8% of theoretical density (TD = 5.78 g cm^{-3}) and 5.50–5.59 g cm^{-3} corresponding to 95.2–96.7% of TD for 2 h. The density of ceramics doped with 1.0 mol % Er_2O_3 exhibited a minimum for both sintering times. On the whole, the ceramics sintered for 2 h were more densified than those sintered for 1 h. This is easily confirmed through the decrease of pores on surface morphology of SEM

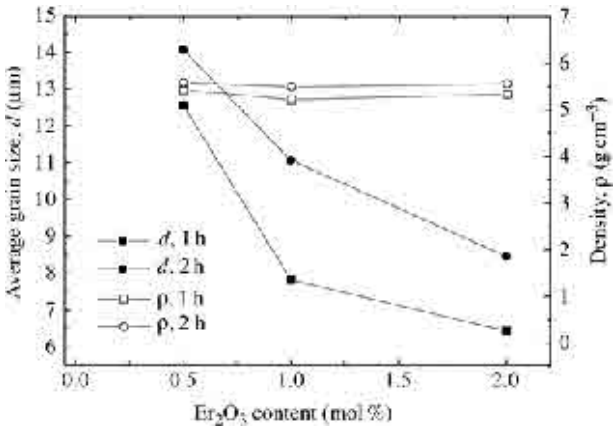

Figure 2 Variation of the average grain size and density of ZPCCE varistor ceramics versus Er_2O_3 content and sintering time.

TABLE I The average grain size (d), density (ρ), shrinkage (S), and porosity (P) of ZPCCE varistor ceramics versus Er_2O_3 content and sintering time

Sintering time (λ)	Er_2O_3 content (mol %)	d (μm)	ρ (g cm^{-3})	S (%)	P (%)
1	0.5	12.6	5.42	18.4	6.2
	1.0	7.8	5.22	16.7	9.7
	2.0	6.4	5.33	17.2	7.8
2	0.5	14.1	5.59	19.2	3.3
	1.0	11.1	5.50	18.6	4.8
	2.0	8.5	5.56	18.7	3.8

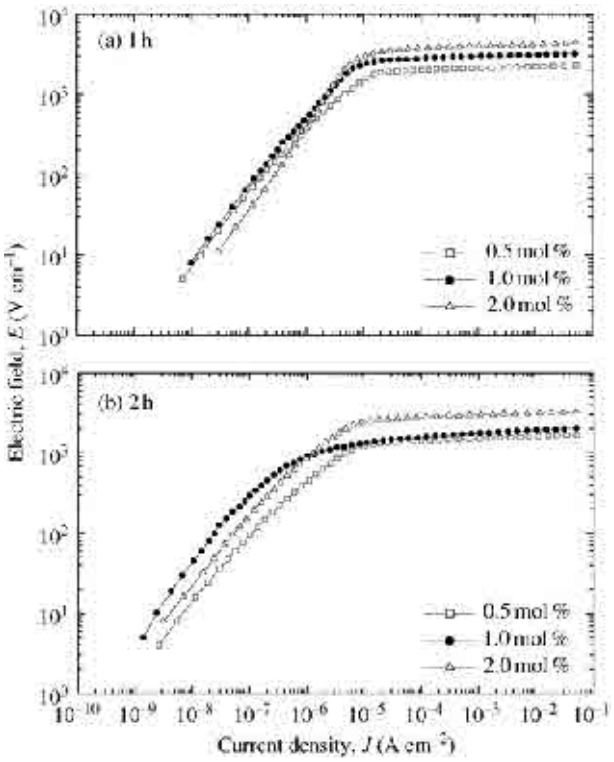

Figure 3 The *E–J* characteristics of ZPCCE varistor ceramics versus Er_2O_3 content and sintering time.

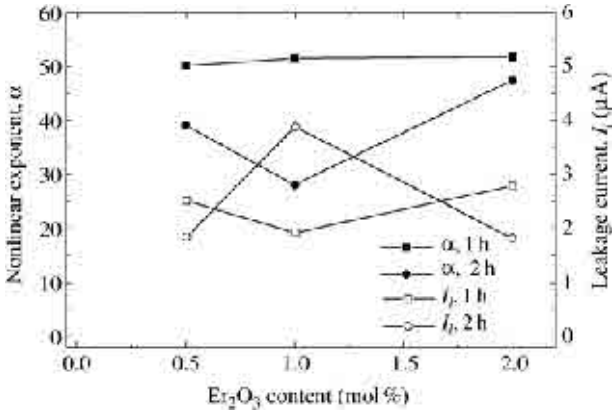

Figure 4 The nonlinear exponent and leakage current of ZPCCE varistor ceramics as a function of Er_2O_3 content with sintering time.

micrographs. The density greatly affects the resistance of degradation, along with a leakage current in the *V–I* characteristics. As we shall discuss later, generally, the larger the density, the higher the stability.

Fig. 3 shows the electric field–current density (*E–J*) characteristic curves of ZPCCE varistor ceramics with Er_2O_3 content and sintering time. For both sintering times, the current density increases linearly in low field, whereas it varies by orders of magnitude with only small changes in field above the breakdown field, called a varistor voltage. It intuitively can be seen that, at the knee region, the *E–J* characteristic curves of varistor ceramics sintered for 1 h are keener than those sintered for 2 h. Therefore, it is believed that the varistor ceramics sintered for 1 h are superior to those sintered for 2 h in the nonlinearity. The variation of *V–I* characteristic parameters, including the varistor voltage ($V_{1\,mA}$), varistor voltage per grain boundary (V_{gb}), nonlinear exponent (α), and leakage current (I_ℓ) are summarized in Table II. With increasing Er_2O_3 content, the $V_{1\,mA}$ and $V_{1\,mA}$ per grain boundary were found to increase in the range of 211.5–396.8 V mm^{-1} for varistor ceramics sintered for 1 h and 153.2–298.6 Vmm^{-1} for 2 h. The $V_{1\,mA}$ is directly related to the number of grain boundaries across a series between the electrodes. Therefore, as Er_2O_3 content is increased, the increase of $V_{1\,mA}$ is attributed to the decrease of average grain size caused by Er_2O_3 addition inhibiting grain growth, as mentioned when discussing microstructure previously. By the same reasoning, it can be seen that the $V_{1\,mA}$ is decreased by a longer sintering time. The V_{gb}, which is a breakdown voltage per grain boundary, is defined as follows: $V_{gb} = (d/D) \cdot V_{1\,mA}$, where d is the average grain size and D is the thickness of the sample. It was in the range of 2.3–2.7 V/gb for the varistor ceramics sintered for 1 h and 2.0–2.5 V/gb for 2 h with Er_2O_3 content. This was within the generally well-known 2–3 V/gb regardless of the sintering processes.

One of the most important figures of merit in varistor ceramics is the nonlinear exponent (α), which characterizes the native properties of varistor itself. Fig. 4 shows the nonlinear exponent (α) and leakage current (I_ℓ) of ZPCCE varistor ceramics as a function of Er_2O_3 content with sintering time. The varistor ceramics sintered for 1 h exhibited high α value above $\alpha = 50$. As Er_2O_3 content is increased, the α value was slightly increased, whereas it was not nearly so affected by Er_2O_3 content. On the other hand, the varistor ceramics sintered for 2 h exhibited low α, compared with those sintered for 1 h. The increase of sintering time in equivalent compositions will lead to the low nonlinearity. However, the stability may be improved due to the increase of ceramic density. The α value varied in a roughly V-shaped manner, reaching a minimum value (28.0) at 1.0 mol %. The maximum value of α was obtained from the varistor ceramics doped with 2.0 mol % Er_2O_3, reaching $\alpha = 47.4$ close to 50. As a result, the Er_2O_3 content dependence of α value of the varistor ceramics sintered for 2 h was found to be

TABLE II The *V–I* and *C–V* characteristic parameters of ZPCCE varistor ceramics versus Er_2O_3 content and sintering time

Sintering time (λ)	Er_2O_3 content (mol %)	$V_{1\,mA}$ (V mm^{-1})	V_{gb} (V/gb)	α	I_ℓ (μA)	N_d (10^{18} cm^{-3})	N_t (10^{12} cm^{-2})	ϕ_b (eV)	t (nm)
1	0.5	211.5	2.7	50.2	2.5	0.94	3.15	1.13	33.54
	1.0	296.8	2.3	51.5	1.9	0.90	2.16	0.55	24.01
	2.0	396.8	2.5	51.7	2.8	0.90	1.94	0.45	21.55
2	0.5	153.2	2.2	39.1	1.8	1.61	3.96	1.04	24.67
	1.0	177.1	2.0	28.0	3.9	1.37	3.59	1.00	26.15
	2.0	298.6	2.5	47.4	1.8	0.88	2.92	1.03	33.15

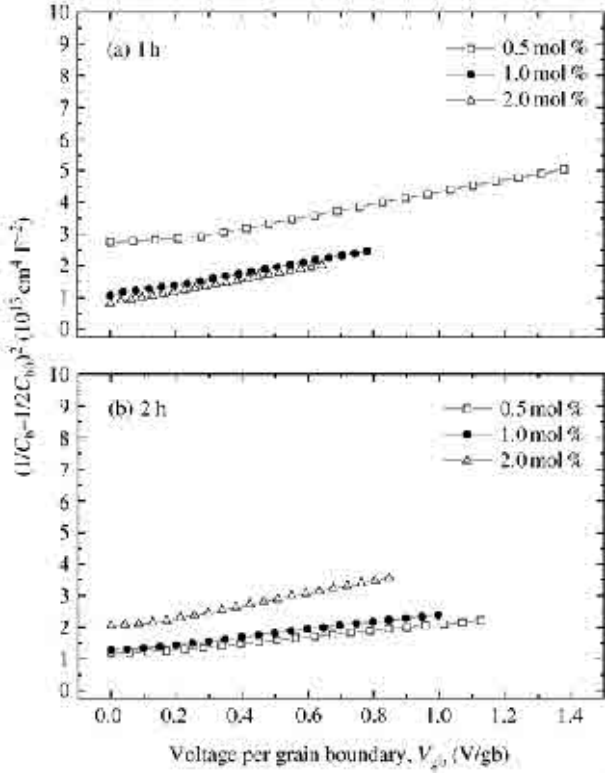

Figure 5 *C–V* characteristics of ZPCCE varistor ceramics versus Er_2O_3 content and sintering time.

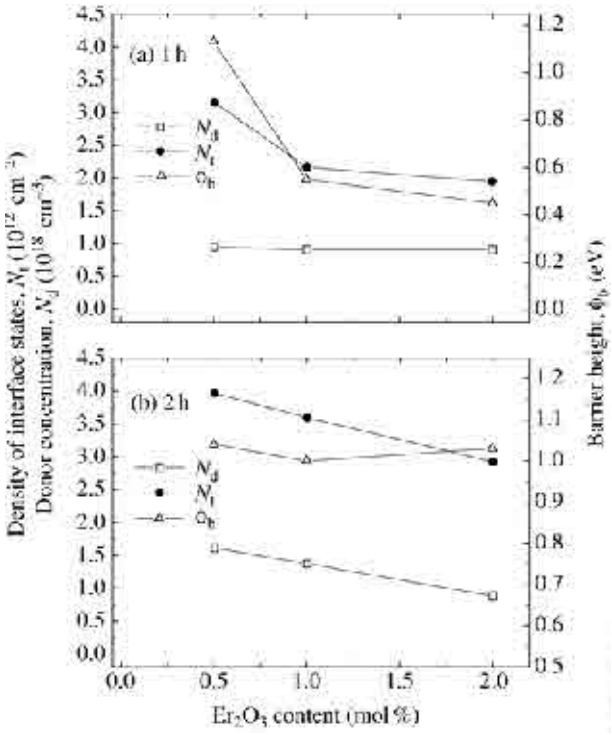

Figure 6 Donor concentration, density of interface states, and barrier height of ZPCCE varistor ceramics as a function of Er_2O_3 content with sintering time.

stronger than that of the varistor ceramics sintered for 1 h. The variation of I_ℓ for the varistor ceramics sintered for 1 h was in the range of 1.9–2.8 μA, with a minimum value at 1.0 mol % Er_2O_3 with increasing Er_2O_3 content and in the range of 1.8–3.9 μA, with a maximum value at 1.0 mol % Er_2O_3 for 2 h. For both sintering times, the minimum value of I_ℓ (1.8 μA) was obtained from the varistor ceramics sintered for 2 h with 2.0 mol % Er_2O_3. It is expected that this ZPCCE varistor ceramics will exhibit a high stability due to the high density and the lowest leakage current.

Fig. 5 shows the *C–V* characteristics of ZPCCE varistor ceramics with Er_2O_3 content and sintering time. It is assumed that the *C–V* characteristics for sintering time will be different because the *C–V* characteristic curves are arranged differently according to Er_2O_3 content and sintering time. The *C–V* characteristic parameters, including the donor concentration (N_d), density of interface states (N_t), barrier height (ϕ_b), and depletion layer width (t) are summarized in Table II. Furthermore, their tendency of variation is shown in Fig. 6. As the Er_2O_3 content is increased, the N_d value of the varistor ceramics sintered for 1 h was nearly constant in the range of 0.94×10^{18}–0.90×10^{18} cm^{-3}, whereas it was found to decrease in the range of 1.61×10^{18}–0.88×10^{18} cm^{-3} for 2 h. These do not greatly differ from the general $\sim 10^{18}$ order of magnitude. The decrease of N_d with Er_2O_3 content exhibited the same tendency as the $ZnO–Pr_6O_{11}–CoO–R_2O_3$ (R = Dy, Er) system with no Cr_2O_3 [12, 13]. This shows that the Er_2O_3 serves as an acceptor. Although Er^{+3} ions have a larger radius (0.088 nm) than Zn^{+2} ions (0.074 nm), thus limited substitution within the ZnO grains is possible. Er substitutes for Zn and creates lattice defects in ZnO grains. The chemical-defects reaction using Kroger–Vink notation can be written as follows:

$$Er_2O_3 \xrightarrow{ZnO} 2Er_{Zn}^{\cdot} + V_{Zn}^{''} + O_O^{\times} + 1/2O_2$$

where $Er_{Zn}^{\cdot}$ is a positively singly charged Er ion substituted for a Zn lattice site, $V_{Zn}^{''}$ is a negatively doubly charged Zn vacancy, and $O_O^{\times}$ is a neutral oxygen on an oxygen lattice site. The oxygen generated in the reaction above affects the donor concentration. In other words, the N_d value is related to the partial pressure of oxygen (P_{O_2}), namely, $N_d \propto P_{O_2}^{-1/4}$ or $P_{O_2}^{-1/6}$. It is, therefore, believed that the decrease of N_d with Er_2O_3 content is attributed to the increase of partial pressure of oxygen. As a result, Er_2O_3 acts as an acceptor. The N_t value was decreased in the range of 3.15×10^{12}–1.94×10^{12} cm^{-2} for the varistor ceramics sintered for 1 h and 3.94×10^{12}–2.92×10^{12} cm^{-2} for 2 h with increasing Er_2O_3 content. The ϕ_b value was decreased in the range of 1.13–0.45 eV for the varistor ceramics sintered for 1 h with increasing Er_2O_3 content, whereas it was nearly constant at about 1 eV for 2 h.

In an application of varistor ceramics, two important factors that should be considered are the nonlinearity and its stability. The electronic equipments and the electrical power systems to be protected from various surges require a high stability of varistor ceramics in order to enhance reliability. In practice, ZnO varistor ceramics begin to degrade because of gradually increasing leakage current with stress time. Eventually, they result in thermal runaway and the loss of varistor function. Therefore, the electrical stability of the varistor ceramics is the most important factor. From this viewpoint, in addition to nonlinearity, the electrical stability is a technologically very important characteristic of ZnO varistor ceramics.

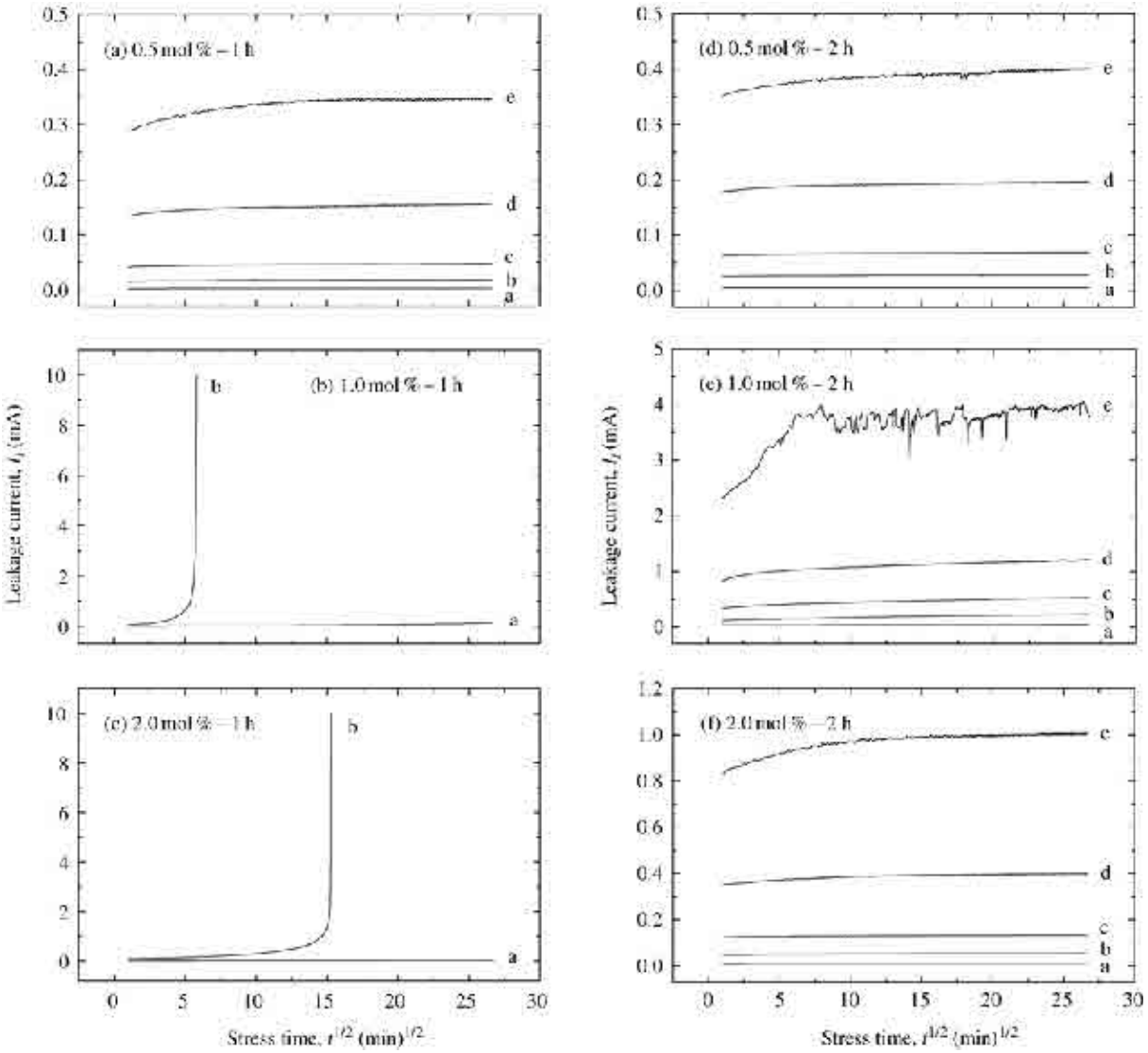

Figure 7 Leakage current of ZPCCE varistor ceramics during various DC accelerated aging stresses with Er_2O_3 content and sintering time; (a) the first stress, (b) the second stress, (c) the third stress, (d) the fourth stress, and (e) the fifth stress.

Fig. 7 shows the leakage current of ZPCCE varistor ceramics during the DC accelerated aging stress versus Er_2O_3 content and sintering time. ZPCCE varistor ceramics doped with 1.0 and 2.0 mol % Er_2O_3 sintered for 1 h exhibited thermal runaway within a short time under the second stress. These varistor ceramics were completely degraded thereafter. This instability is attributed to the low density, that is, the low density leads to the concentration of current through the limited conduction path and further high current density per grain boundary. This means that the density more predominantly affects the stability, compared with the leakage current. On the contrary, it can be seen that the varistor ceramics doped with 0.5 mol % Er_2O_3 sintered for 1 h exhibit remarkably high stability compared with the varistor ceramics with 1.0 and 2.0 mol % Er_2O_3. Their leakage current was nearly constant until the fourth stress and shows very weak positive creep during the fifth stress.

On the other hand, in the varistor ceramics sintered for 2 h, the stability of varistor ceramics doped with 1.0 and 2.0 mol % Er_2O_3 was remarkably enhanced with no thermal runaway, compared with those for 1 h. The estimation for stability cannot be confirmed directly from $I_\ell - t^{1/2}$ curves. Therefore, the variation of *V–I* characteristic parameters for only varistor ceramics with no thermal runaway after various DC accelerated aging stresses is shown in Fig. 8. Furthermore, the detailed variation rate of *V–I* characteristic parameters is summarized in Table III. The varistor ceramics with 0.5 mol % Er_2O_3 sintered for 2 h revealed a higher stability, with $\%\Delta V_{1\,mA}$ (variation rate of $V_{1\,mA}$) of -1.76%, $\%\Delta\alpha$ (variation rate of α) of -4.35%, and $\%\Delta I_\ell$ (variation rate of I_ℓ) of $+244.44\%$ after the fifth stress. The stability of the nonlinear exponent and leakage current was found to be well above twice those sintered for 1 h. Er_2O_3-doped Pr_6O_{11}-based ZnO varistor ceramics studied so far have exhibited the best performance at 0.5 mol % Er_2O_3 with respect to densification and electrical stability. An interesting point is that the varistor ceramics sintered at 1345 °C for 2 h revealed the best performance at 2.0 mol % Er_2O_3. This is clearly different from the existing results. The variation rate of the *V–I* characteristic parameters of this varistor ceramic is small compared with others, as can be seen in Fig. 8. It should be emphasized that this varistor ceramics exhibit very high stability, in which $\%\Delta V_{1\,mA} = -0.54\%, \%\Delta\alpha = -4.01\%$, and $\%\Delta I_\ell = +155.56\%$ even after the fifth stress. In particular, $\%\Delta V_{1\,mA}$ was less than only 1%. In general,

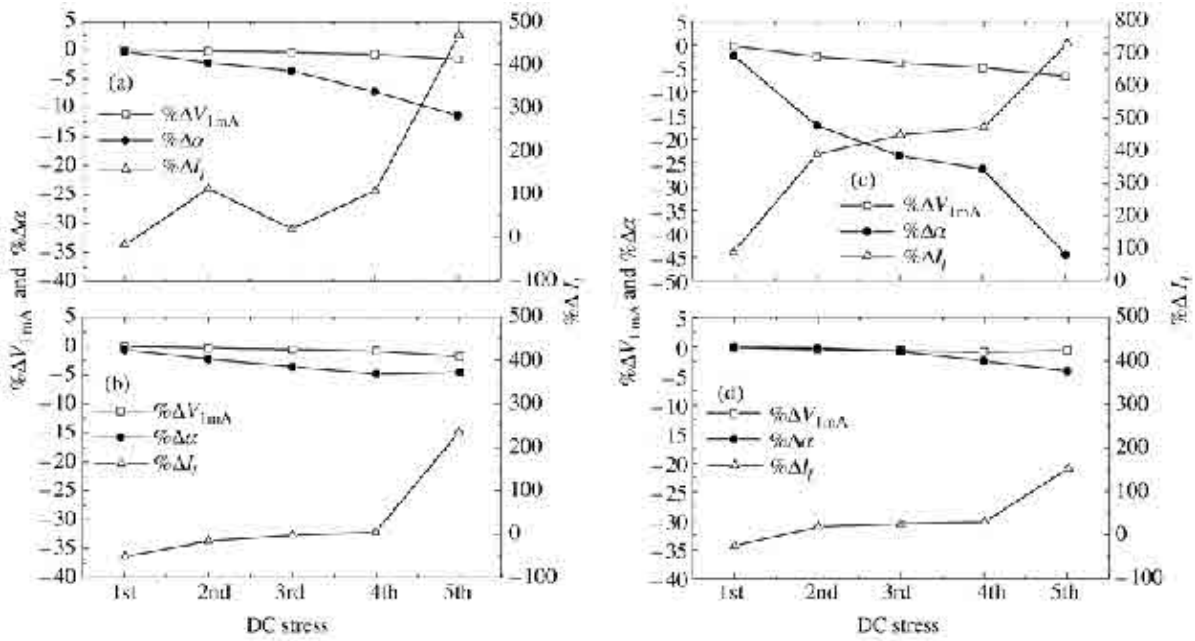

Figure 8 Variation rate of *V–I* characteristic parameters as a function of DC accelerated aging stress of ZPCCE varistor ceramics with no thermal runaway; (a) 0.5 mol % − 1 h, (b) 0.5 mol % − 2 h, (c) 1.0 mol % − 2 h, and (d) 2.0 mol % − 2 h.

TABLE III Variation of *V–I* characteristic parameters of ZPCCE varistor ceramics after various DC accelerated aging stresses with Er_2O_3 content and sintering time

Sintering time (λ)	Er_2O_3 content (mol %)	Stress state	$V_{1\,mA}$ ($V\,mm^{-1}$)	$\%\Delta V_{1\,mA}$	α	%Δα	I_ℓ (μA)	$\%\Delta I_\ell$
1	0.5	Before	211.5	0	50.2	0	2.5	0
		1st	211.5	0	50.0	− 0.40	2.1	− 16.0
		2nd	210.9	− 0.28	49.0	− 2.39	5.3	112.0
		3rd	210.6	− 0.42	48.4	− 3.59	3.0	20.0
		4th	209.8	− 0.80	46.5	− 7.37	5.2	108.0
		5th	208.0	− 1.65	44.5	− 11.35	14.3	472.0
	1.0	Before	296.8	0	51.5	0	1.9	0
		1st	297.0	0.07	46.4	− 9.90	3.6	89.47
		2nd	Thermal runaway					
	2.0	Before	396.8	0	51.7	0	2.8	0
		1st	402.0	1.31	48.8	− 5.61	4.0	42.86
		2nd	Thermal runaway					
2	0.5	Before	153.2	0	39.1	0	1.8	0
		1st	153.1	− 0.07	38.9	− 0.51	0.9	− 50.0
		2nd	152.7	− 0.33	38.2	− 2.30	1.5	− 16.67
		3rd	152.3	− 0.59	37.7	− 3.58	1.8	0
		4th	151.8	− 0.91	37.2	− 4.86	1.9	5.55
		5th	150.5	− 1.76	37.4	− 4.35	6.2	244.44
	1.0	Before	177.1	0	28.0	0	3.9	0
		1st	176.5	− 0.34	27.3	− 2.50	7.3	87.18
		2nd	172.6	− 2.54	23.2	− 17.14	19.0	387.18
		3rd	170.3	− 3.84	21.4	− 23.57	21.3	446.15
		4th	168.4	− 4.91	20.6	− 26.43	22.2	469.23
		5th	165.3	− 6.66	15.6	− 44.29	32.2	725.64
	2.0	Before	298.6	0	47.4	0	1.8	0
		1st	298.3	− 0.10	47.4	0	1.4	− 22.22
		2nd	297.5	− 0.37	47.3	− 0.21	2.2	22.22
		3rd	296.9	− 0.57	47.1	− 0.63	2.3	27.78
		4th	296.1	− 0.84	46.3	− 2.32	2.4	33.33
		5th	297.0	− 0.54	45.5	− 4.01	4.6	155.56

the stability for DC accelerated aging stress is high, as the ceramics are densified and the leakage current is lowered. Although the varistor ceramics with 0.5 and 2.0 mol % Er_2O_3 have nearly the same density and leakage current, what is why the latter exhibit a higher stability than the former?

A grain-boundary-defect model has been developed to demonstrate instability in ZnO varistor ceramics [22]. The likely proper degradation phenomenon is ascribed to the migration of mobile zinc interstitials (Zn_i) within the depletion layer toward grain boundaries. The Zn_i is diffused by the biasing field and successively reacts with grain-boundary defects. As a result, this process leads to a reduction of the potential barrier and an increase of

leakage current. Therefore, the way to improve the stability is to restrict the generation of Zn_i within the depletion layer or the migration of Zn_i toward grain boundaries. It is well known that the presence of Na^+ and Ag^+ hinders the migration of Zn_i, effectively increasing the apparent migration activation energies of Zn_i. Ultimately, these ions improve the stability [23, 24]. These ions are larger than Zn^+ and exist as interstitial ions. The Er^{3+} ion is also larger than the Zn^{2+} ion. Assuming added Er_2O_3 exists in Er_i sites within the depletion layer, it may also decrease the concentration of Zn_i. As a result, since the higher Er_2O_3 content lead to the low concentration of Zn_i, it is believed this explains why the varistor with 2.0 mol % Er_2O_3 sintered for 2 h exhibit a high stability, compared with those of 0.5 mol %.

4. Conclusions

The electrical properties and their stability for DC accelerated aging stress of ZPCCE varistor ceramics, which are composed of ZnO–Pr_6O_{11}–CoO–Cr_2O_3–Er_2O_3 systems, were investigated versus Er_2O_3 content and sintering time. The density of varistor ceramics was increased with increasing sintering time, whereas it decreased with increasing Er_2O_3 content. In the varistor ceramics sintered for 1 h, as Er_2O_3 content is increased, it was found that the nonlinear exponent is nearly constant, close to 50, and the leakage current varies with a V-shape, reaching a minimum value (1.9 μA) at 1.0 mol %. The varistor ceramics sintered for 2 h exhibited the best nonlinear properties at 2.0 mol % Er_2O_3, with a maximum value (47.4) of the nonlinear exponent and a minimum value (1.8 μA) of the leakage current. A longer sintering time decreased the nonlinear properties, whereas it greatly improved the stability against DC accelerated aging stress in the equivalent Er_2O_3 content. In particular, the varistor ceramics doped with 2.0 mol % Er_2O_3 sintered for 2 h exhibited an excellent stability, in which $\%\Delta V_{1\,mA} = -0.54\%$, $\%\Delta\alpha = -4.01\%$, and $\%\Delta I_\ell = +155.56\%$ after the fifth stress, under severe DC stress such as $(0.80_{1\,mA}/90°C/12\,h) + (0.85\,V_{1\,mA}/115°C/12\,h) + (0.90\,V_{1\,mA}/120°C/12\,h) + (0.95\,V_{1\,mA}/125°C/12\,h) + (0.95\,V_{1\,mA}/150°C/12\,h)$. Consequently, it was estimated that the varistor ceramics will be applied to surge absorbers and arresters having high performance and high stability in the future.

Acknowledgments

This work was supported by ECC (Electronic Ceramics Center) at Dongeui University as RRC · TIC program through KOSEF (Korea Science and Engineering Foundation), ITEP (Korea Institute of Industrial Technology Evaluation and Planning), and Busan Metropolitan City.

References

1. L. M. LEVINSON and H. R. PILIPP, *Am. Ceram. Soc. Bull.* **65** (1986) 639.
2. T. K. GUPTA, *J. Am. Ceram. Soc.* **73** (1990) 1817.
3. H. R. PILIPP and L. M. LEVINSON, *J. Appl. Phys.* **46** (1976) 1332.
4. D. R. CLARKE, *J. Am. Ceram. Soc.* **82** (1999) 485.
5. Y. S. LEE and T. Y. TSENG, *ibid.* **75** (1992) 1636.
6. A. B. ALLES and V. L. BURDICK, *J. Appl. Phys.* **70** (1991) 6883.
7. A. B. ALLES, R. PUSKAS, G. CALLAHAN and V. L. BURDICK, *J. Am. Ceram. Soc.* **76** (1993) 2098.
8. Y.-S. LEE, K.-S. LIAO and T.-Y. TSENG, *ibid.* **79** (1996) 2379.
9. C.-W. NAHM, C.-H. PARK and H.-S. YOON, *J. Mater. Sci. Lett.* **19** (2000) 271.
10. C.-W. NAHM and C.-H. PARK, *J. Mater. Sci.* **35** (2000) 3037.
11. C.-W. NAHM, C.-H. PARK and H.-S. YOON, *J. Mater. Sci. Lett.* **19** (2000) 725.
12. C.-W. NAHM, *J. Eur. Ceram. Sci.* **21** (2001) 545.
13. C.-W. NAHM and C.-H. PARK, *J. Mater. Sci.* **36** (2001) 1671.
14. C.-W. NAHM, *Mater. Lett.* **47** (2001) 182.
15. C.-W. NAHM, H.-S. YOON and J.-S. RYU, *J. Mater. Sci. Lett.* **20** (2001) 393.
16. C.-W. NAHM and J.-S. RYU, *Mater. Lett.* **53** (2002) 110.
17. C.-W. NAHM and B.-C. SHIN, *J. Mater. Sci.: Mater. Electron* **13** (2002) 111.
18. C.-W. NAHM, *J. Mater. Sci. Lett.* **21** (2002) 201.
19. M. MUKAE, K. TSUDA and I. NAGASAWA, *J. Appl. Phys.* **50** (1979) 4475.
20. L. HOZER, in ''Semiconductor Ceramics: Grain Boundary Effects'' (Ellis Horwood, 1994) p. 22.
21. J. C. WURST and J. A. NELSON, *J. Am. Ceram. Soc.* **55** (1972) 109.
22. T. K. GUPTA and W. G. CARLSON, *J. Mater. Sci.* **20** (1985) 3487.
23. J. FAN and R. FREER, *J. Appl. Phys.* **77** (1995) 4795.
24. D. J. BINKS R. W. GRIMES and D. L. MORGENSTEIN, *Br. Ceram. Proc.* **52** (1994) 159.

Received 19 August 2002
and accepted 26 March 2003